THE ASTROPHYSICAL JOURNAL, 458:467–473, 1996 February 20

SPECTROSCOPY OF H II REGIONS IN M81 GROUP DWARF GALAXIES

BRYAN W. MILLER[1,2] AND PAUL HODGE[1]
Astronomy Department, University of Washington, Seattle, WA 98195
Received 1995 June 22; accepted 1995 August 23

ABSTRACT

We present nebular spectroscopy of H II regions in the M81 Group irregular galaxies M81dB, Ho I, and IC 2574. The empirical, or bright line, method is used to determine the oxygen abundances and ionization parameters. When the [O III] λ4363 line is detected, the directly calculated oxygen abundances agree with the empirical values within the uncertainties. The oxygen abundances are typically $\sim$0.12 solar and are consistent with the log (O/H)–M_B relation. Nitrogen abundances are also normal for irregular galaxies.

Subject headings: galaxies: abundances — galaxies: clusters: individual (M81) — galaxies: irregular — galaxies: ISM — H II regions

1. INTRODUCTION

Dwarf galaxies are prime objects for the study of the evolution of galaxies because of their relatively simple kinematics, low dust content, and large numbers in the local universe (Gallagher & Hunter 1984). Dwarf galaxies generally have abundances between 3% and 20% of the solar values (see Skillman, Kennicutt, & Hodge 1989, hereafter SKH, and references therein). This may be a result of their low masses, which gives them much less gas out of which to form stars, and which may not allow them to retain the gas that they have, or of their low and variable star formation rates. Some dwarfs, such as I Zw 18 (Kunth & Sargent 1986) may have formed in the last few billion years and may be undergoing only their second or third epoch of star formation. The relative abundances of important elements such as carbon, nitrogen, oxygen, and iron in dwarf galaxies also differ from those of the larger star-forming galaxies (Garnett 1990; Garnett et al. 1995) and Gilmore & Wyse (1991) have discussed how these relative abundance ratio variations can be tied to differences in star formation histories. Knowledge of the abundances in dwarfs is an important constraint on evolutionary models and the correct interpretation of global colors and color-magnitude diagrams. Thus, dwarf galaxies give us an opportunity to study the process of star formation in conditions that are different from those in our Galaxy at present.

Abundance studies in dwarf galaxies are also relevant to the problem of determining the primordial helium abundance, which is a constraint to theories of the origin of the universe. It is usually determined by extrapolating the observed trend of He/H with O/H to zero oxygen or nitrogen abundance (Pagel et al. 1992). Helium abundances from very low metallicity dwarf galaxies tie down the low-abundance end of the extrapolation (see Shields 1990; Skillman et al. 1993). SKH emphasized that surveying the H II regions in low-luminosity galaxies is a good technique for finding low-abundance H II regions that are useful for addressing the primordial abundance question.

We have been involved in a long-term program to compile Hα fluxes and oxygen abundances for a complete sample of nearby dwarf irregular galaxies in order to study their star formation histories (see SKH; Miller & Hodge 1994, and references therein; Hodge & Miller 1995). Miller & Hodge (1994, hereafter MH94) presented Hα imaging and star formation rates for M81dA, M81dB, Ho I, Ho IX, and IC 2574 in the M81 Group. This paper presents long-slit spectroscopy and derived oxygen abundances of the brightest H II regions in three of these galaxies: M81dB, Ho I, and IC 2574. M81dA did not have detectable H II regions. Spectroscopy of a possible supernova remnant near Ho IX is presented in Miller (1995). The observations are described in § 2, the method for determining the oxygen and nitrogen abundances is discussed in § 3, and, finally, the results are discussed and summarized in § 4.

2. OBSERVATIONS AND DATA REDUCTION

2.1. *Observations*

Observations of the H II regions in the M81 dwarfs were acquired on 1993 September 17–19 (UT) with the KPNO 2.1 m telescope and a Ford 1024 × 3072 pixel CCD in the Gold spectrograph. Grating 240 was used to give wavelength coverage from 3100 to 7600 Å with a resolution of about 6 Å. The usable wavelength range is from about 3500 to 7000 Å. A WG 345 order sorting filter was used to minimize contamination from the second order spectrum. Weather conditions on these nights were spectroscopic; all the observations were done through fairly thick cloud cover. Absolute fluxes that are given should not be used quantitatively, though, assuming that clouds are gray absorbers, the line ratios should be usable for our purposes. Observations of the IRS standard stars Fiege 34, BD +28°4211, and Hiltner 102 provided sensitivity calibration. Total integration times for the program objects were about 1 hr.

The only H II region that was visible on the acquisition TV monitor was 167 in IC 2574. In that case, the slit was centered on the brightest emission. For the rest of the observations, the target was acquired by doing blind offsets from nearby stars. Offsets were determined using the H II region astrometry from MH94. As a result of astrometric and pointing errors, there is a 2″–4″ uncertainty in the location of the slit with respect to the center of the H II region. A 4″ slit was used as a compromise between good spectral resolution and getting as much of the

[1] Visiting Astronomer, Kitt Peak National Observatory, which is operated by AURA, Inc., under contract with the NSF.
[2] Currently at Department of Terrestrial Magnetism, 5241 Broad Branch Road NW, Washington, DC 20015, and Space Telescope Science Institute, 3700 San Martin Drive, Baltimore, MD 21218.

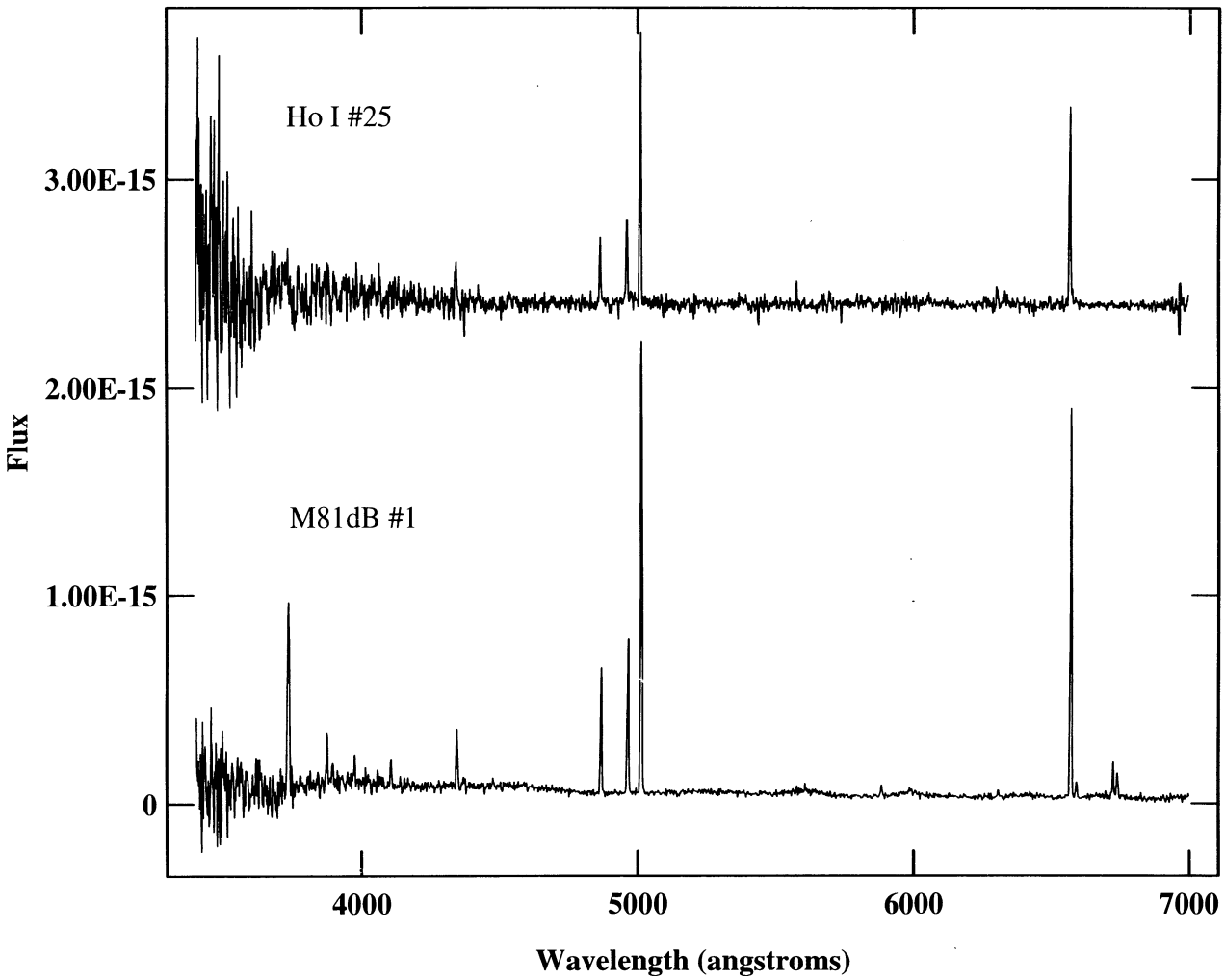

FIG. 1.—KPNO 2.1 m spectra of Ho I MH 25 and M81dB MH 1. The Ho I spectrum as been scaled by a factor of 3 for display because of clouds during observation.

H II region as possible into the slit. A wide, 10″ slit was used to observe all standard stars in order to minimize slit loss that would add systematic error to the sensitivity calibration.

2.2. *Data Reduction*

Pixel-to-pixel sensitivity variations were corrected using quartz flats with an illumination correction from twilight flats. Cosmic rays in the CCD frames were removed by hand using the IRAF[3] task *imedit*. Any cosmic rays falling near emission lines were left in the two-dimensional image. They were removed later by a sigma-clipping algorithm when separate spectra of the sample object were averaged together. Wavelength calibration was done using comparison arcs bracketing each object frame. Extracted standard star spectra were then used to determine the sensitivity with wavelength. A residual extinction correction was also applied in cases where it was statistically significant. This helped to improve the agreement between the observed and theoretical Balmer line ratios.

Because of weak continuum emission from the H II regions, their spectra could not be traced over the length of the detector. Instead, the shape of a well traced standard star was used as a template when extracting each H II region spectrum. The width of the extraction was defined by the width of the Hβ line. Individual extracted spectra of a given object were then flux calibrated and averaged together. Spectra that had only been dispersion corrected were also summed to form a spectrum suitable for determining the photon statistics for each line. Fluxes for the lines were determined from Gaussian fits to the line profiles. Three independent measurements were made of each line and the results averaged to produce the final flux measurement. The final spectra are shown in Figures 1 and 2.

Reddening corrected line ratios $I(\lambda)/I(\mathrm{H}\beta)$ are given in Table 1. The ratios were corrected for Galactic and internal reddening using the equation

$$\frac{I(\lambda)}{I(\mathrm{H}\beta)} = \frac{F(\lambda)}{F(\mathrm{H}\beta)}\, 10^{c(\mathrm{H}\beta)f(\lambda)} \qquad (1)$$

where $I(\lambda)$ is the intrinsic line flux, $F(\lambda)$ is the observed line flux, $c(\mathrm{H}\beta)$ is the logarithmic reddening correction at Hβ, and $f(\lambda)$ is

[3] IRAF is distributed by the National Optical Astronomy Observatories, which is operated by the Association of Universities for Research in Astronomy, Inc., under cooperative agreement with the National Science Foundation

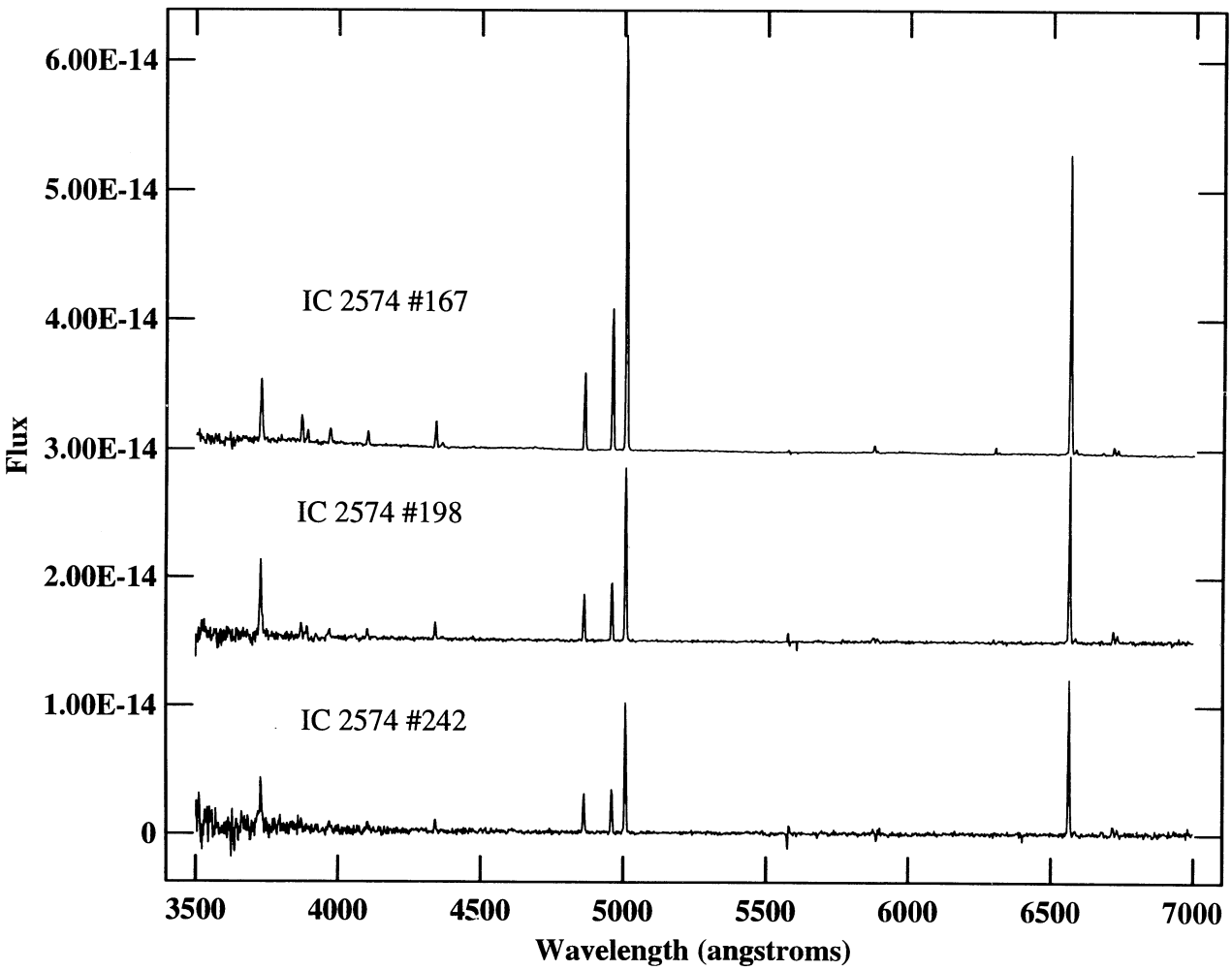

FIG. 2.—KPNO 2.1 m spectra of IC 2574 MH 167, MH 198, MH 242. The spectra have been offset by 2×10^{-14} erg s^{-1} cm^{-2} Å^{-1}.

the Galactic reddening function, normalized to Hβ. The reddening function was taken from the Galactic reddening law of Seaton (1979) using the analytic expression of Howarth (1983), assuming a value of $R = A_V/E(B-V) = 3.1$. The quantity $C(\mathrm{H}\beta)$ was determined from the observed Balmer line ratios after correcting for 2 Å equivalent width of underlying stellar absorption. Intrinsic Balmer line ratios were found by interpolating the values from Brocklehurst (1971) to an electron temperature of 15,000 K. The fractional uncertainties in the line strengths were calculated using standard error propagation based on photon counting statistics (see Skillman & Kennicutt 1993; Skillman et al. 1994). The derived values and uncertainties of $c(\mathrm{H}\beta)$ are also given in Table 1.

3. OXYGEN AND NITROGEN ABUNDANCES

3.1. *Electron Densities, Temperatures, and the Direct Method*

Electron densities were calculated using the [S II] λ6717:λ6731 ratio when those lines were detected. The ratios all have uncertainties ranging from 30% to over 50% so the derived density for a given H II region is not very useful. However, all the ratios are consistent with the canonical value of 100 cm^{-3}, and that value was adopted in all further calculations.

Spectra of the brightest H II regions had detections of [O III] λ4363, which allows use of the direct method for determining the temperature in the O^{++} region. The five-level atom program FIVEL (De Robertis, Dufour, & Hunt 1987) was used to calculate $T_e(O^{++})$ given the observed $[I(4959) + I(5007)]/I(4363)$ ratios and $N_e = 100$. The results are shown in the first row of Table 2. The value of $1.44 \pm 0.15 \times 10^4$ K for 167 in IC 2574 agrees within the error with $T_e = 1.34 \times 10^4$ K from Drissen, Roy, & Moffat (1993). We assumed a temperature of 1.5×10^4 K for those H II regions without an [O III] λ4363 measurement.

Models indicate that the electron temperature in the O^{++} zone can be substantially different from the temperature in the O^+ zone (Stasińska 1982). The following relation from Pagel et al. (1992) is used to estimate the temperature in the O^+ zone:

$$T_4(O^+) = 2[T_4^{-1}(O^{++}) + 0.8]^{-1}, \quad (2)$$

where T_4 is the electron temperature in units of 10^4 K. Skillman & Kennicutt (1993) show that this relation agrees with the H II region models of Stasińska (1990) and Skillman (1989). For the H II regions with independently derived temperatures, those temperatures were used to determine the emissivities of the lines using the FIVEL program. The ionic and total abundances can then be derived, and the results are given in the second, third, and fourth rows of Table 2.

TABLE 1

LINE RATIOS FOR Ho I, M81dB, AND IC 2574

Object	Ho I 25	M81dB 1	IC 2574 167	IC 2574 198	IC 2574 242
3727 [O II]	$<0.8 \pm 1.1$	2.00 ± 0.44	1.32 ± 0.25	2.80 ± 0.52	2.56 ± 0.48
3868 [Ne III]	...	0.35 ± 0.16	0.48 ± 0.09	0.46 ± 0.09	0.30 ± 0.06
3889 H 8 + He I	...	0.14 ± 0.14	0.17 ± 0.04	0.29 ± 0.06	...
3968 H 7 + [Ne III]	...	0.17 ± 0.10	0.30 ± 0.06	0.29 ± 0.06	0.40 ± 0.08
4101 Hδ	...	0.25 ± 0.12	0.28 ± 0.05	0.29 ± 0.06	0.40 ± 0.07
4340 Hγ	0.88 ± 0.28	0.48 ± 0.11	0.44 ± 0.07	0.46 ± 0.07	0.44 ± 0.07
4363 [O III]	...	0.07 ± 0.06	0.09 ± 0.02	...	...
4471 He I	...	0.06 ± 0.05	...	...	...
4861 Hβ	1.00 ± 0.21	1.00 ± 0.17	1.00 ± 0.14	1.00 ± 0.14	1.00 ± 0.14
4959 [O III]	1.27 ± 0.25	1.19 ± 0.20	1.68 ± 0.24	1.19 ± 0.17	1.03 ± 0.14
5007 [O III]	3.87 ± 0.62	3.51 ± 0.58	4.95 ± 0.71	3.59 ± 0.52	3.14 ± 0.45
5876 He I	...	0.09 ± 0.09	0.06 ± 0.01	...	...
6548 [N II]	...	...	0.01 ± 0.01	...	...
6563 Hα	2.75 ± 0.62	2.66 ± 0.61	2.56 ± 0.52	2.75 ± 0.56	2.34 ± 0.48
6584 [N II]	0.12 ± 0.12	0.11 ± 0.06	0.04 ± 0.01	0.08 ± 0.02	0.08 ± 0.02
6678 He I	...	...	0.02 ± 0.01	...	...
6717 [S II]	...	0.22 ± 0.07	0.06 ± 0.01	0.17 ± 0.04	0.14 ± 0.08
6731 [S II]	...	0.18 ± 0.06	0.04 ± 0.01	0.12 ± 0.03	0.08 ± 0.02
$c(\mathrm{H}\beta)$	0.1 ± 0.2	0.15 ± 0.2	0.5 ± 0.2	0.5 ± 0.2	0.7 ± 0.2
$EW(\mathrm{H}\beta)$	166	80	88	136	128
log (R_{23})	0.77 ± 0.10	0.83 ± 0.05	0.90 ± 0.04	0.88 ± 0.04	0.83 ± 0.04
log ([O III]/[O II])	0.8 ± 0.6	0.4 ± 0.1	0.7 ± 0.1	0.2 ± 0.09	0.2 ± 0.1
log ([O III]/[N II])	1.6 ± 0.5	1.6 ± 0.2	2.1 ± 0.1	1.7 ± 0.1	1.7 ± 0.1
log ([N II]/[O II])	-0.8 ± 0.8	-1.26 ± 0.25	-1.52 ± 0.13	-1.55 ± 0.13	-1.51 ± 0.13

3.2. *Distinguishing the Branches of the R_{23} Relation*

The bright-line method proposed by Pagel et al. (1979) must be used to estimate the oxygen abundances of the remaining H II regions. This is complicated by the fact that O/H is double-valued for a given value of R_{23} in the region of low oxygen abundance (Fig. 3). The models of Skillman (1989) and McGaugh (1991) also show that the empirically derived abundances also depend on the ionization of the nebulae. The derived value of the volume-averaged ionization parameter, U, also depends on the branch that is chosen (McGaugh 1991).

One diagnostic that has been used in the past (see, e.g., Hunter & Gallagher 1985) for distinguishing the upper and lower branches is the excitation of the H II region as measured by the ratio log ([O II]/[O III]). Models of H II regions show that [O II]/[O III] decreases with increasing effective stellar temperature or U for a given oxygen abundance (Skillman 1989). As shown in Figure 4, there is a trend of log ([O II]/[O III]) with abundance for $12 + \log(\mathrm{O/H}) > 8.0$ (i.e., on the upper branch). However, the additional directly determined oxygen abundances in low-metallicity H II regions accumulated over the last 10 years show a large scatter in [O II]/[O III] versus O/H. Therefore, one cannot determine the abundance or the branch of the R_{23} relation from the excitation alone.

Another traditional method of resolving the ambiguity between the lower and upper branches of the R_{23} relation is through the [O III] λ5007/[N II] λ6584 ratio. Edmunds & Pagel (1984, hereafter EP) show that this ratio varies by an order of magnitude through the "elbow" of the R_{23} relation. However, the low-abundance end of the O/H–[O III]/[N II] relation shown in Figure A1b of EP is populated by only 4 observational points, one of which falls well off the model predictions. Most of the values of log ([O III]/[N II]) shown in Table 1 are between 1.6 and 2.1, which according to EP, would put them all either on the upper branch or just at the bend in the elbow.

One problem with using [O III]/[N II] for determining the branch of the R_{23} relation is that the [O III] lines are very sensitive to the excitation, or ionization, of the nebula. McGaugh (1994) has proposed using [N II] λ6584/[O II] λ3727 instead. This ratio is less sensitive to U, since the two ions have similar ionization potentials. [N II]/[O II] is dependent on the N/O ratio, limiting it's usefulness as an abundance indicator and possibly weakening its ability to distinguish the branches.

TABLE 2

DERIVED PROPERTIES FROM H II REGION SPECTRA[a]

Property	Ho I 25	M81dB 1	IC 2574 167	IC 2574 198	IC 2574 242
$T(\mathrm{O}^{++}) \times 10^4$	1.5	1.55 ± 1.2	1.44 ± 0.15	1.5	1.5
$\mathrm{O}^{+}/\mathrm{H} \times 10^{-5}$	...	~ 2.3	1.6 ± 0.4	...	...
$\mathrm{O}^{++}/\mathrm{H} \times 10^{-5}$	...	~ 7.2	12.3 ± 1.8	...	...
O/H	...	9.5 ± 4.5	14.0 ± 3.6	...	...
$(\mathrm{O/H})_{\mathrm{LB}} \times 10^{-5}$	$5^{+5}_{-2.5}$	7.9 ± 1.8	10.0 ± 2.3	11 ± 2.3	10.0 ± 2.3
$(\mathrm{O/H})_{\mathrm{UB}} \times 10^{-5}$	59^{+60}_{-30}	45 ± 5	40 ± 5	40 ± 5	45 ± 5
log (U)	-2	-2.5 ± 0.1	-2.1 ± 0.1	-2.5 ± 0.1	-2.6 ± 0.1
log (N/O)	-0.8 ± 0.8	-1.26 ± 0.25	-1.52 ± 0.13	-1.55 ± 0.13	-1.51 ± 0.13
$E(B-V)$	0.1 ± 0.1	0.1 ± 0.1	0.3 ± 0.1	0.3 ± 0.1	0.5 ± 0.1

[a] $N_e = 100\ \mathrm{cm}^{-3}$, temperatures without uncertainties are assumed values.

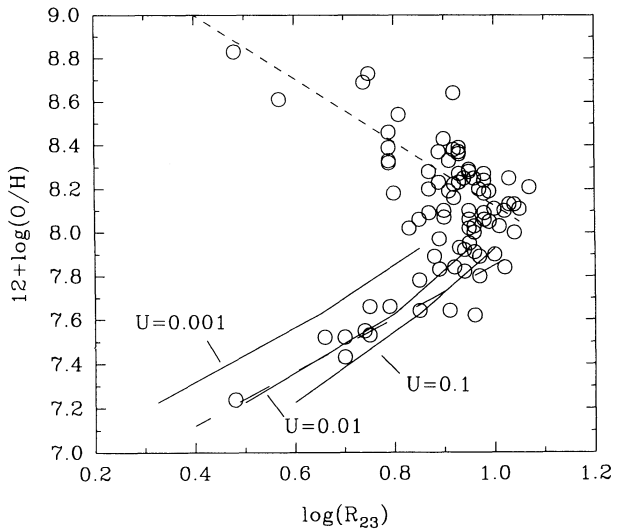

FIG. 3.—Oxygen abundances derived from [O III] λ4363 measurements versus log (R_{23}) in the vicinity where the relation is double valued. Data points are as compiled in McGaugh (1991) with the addition of UGC 4483 from Skillman et al. (1994). The long-dashed line is the lower branch calibration of Skillman (1989). The short-dashed line is the upper branch calibration of Edmunds & Pagel (1984). Solid lines are models from Skillman (1989) showing how abundance depends on the ionization parameter U for the lower branch.

However, Garnett (1990) has shown that N/O is roughly constant with O/H in irregular galaxies over the range $7.2 < 12 + \log(\mathrm{O/H}) < 8.3$. Therefore, for practical purposes [N II]/[O II] is monotonic with O/H, at least enough so that this ratio can distinguish the branches of the R_{23} relation. The division between the upper and lower branches is fairly well defined, with lower branch objects having log ([N II]/[O II]) $\lesssim -1$ (see Fig. 3 of McGaugh 1994). The values of log ([N II]/[O II]) for the H II regions in this study are typically around -1.5, indicating that they fall on the lower branch (see Table 1).

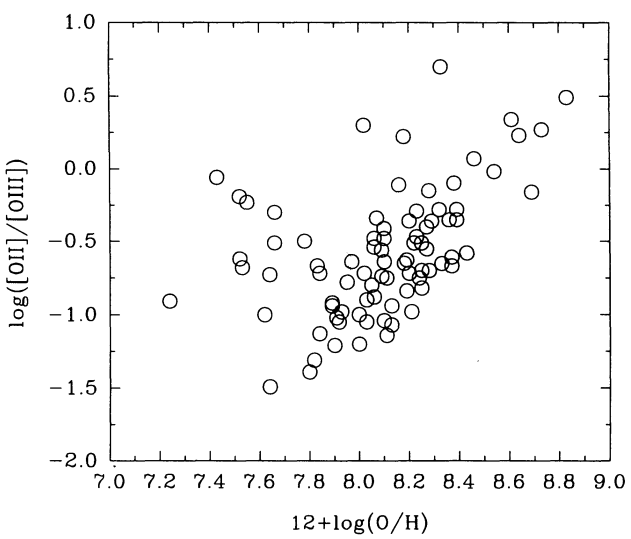

FIG. 4.—Relationship between log ([O II]/[O III]) and 12 + log (O/H) for the same sample of H II regions as in Fig. 3.

3.3. *Ionization and* O/H *from the Empirical Method*

Values for the ionization parameter and the oxygen abundance for the H II regions were determined from log ([O III]/[O II]) and log (R_{23}) using the model grid of McGaugh (1991) as plotted in Figure 2 of McGaugh (1994). The H II regions in this study fall in the same region of the log ([O III]/[O II]), log (R_{23}) plane as the low-abundance H II regions in the low surface brightness galaxies studied by McGaugh (1994)—compare Figure 5 with Figure 2 of McGaugh (1994)—so that model seems to be appropriate for this data. The values of log (U) are shown in the seventh row of Table 2. The range of log ([O III]/[O II]) values lie between 0.2 and 0.7, yielding ionization parameters, U, between 0.008 and 0.003. This range of excitations is a bit low for the abundance but the H II regions in many other nearby dIrr exhibit similar behavior (see Skillman et al. 1988; SKH). To show the differences between abundances calculated using the upper and lower branches of the R_{23} relation, abundances have been determined for both branches, and these are shown in the fifth and sixth rows of Table 2. The percent error ranges between 25% and 50%. Abundances determined in this manner, accounting for the ionization, are typically a factor of 2 higher than found when using the lower branch calibration of Skillman (1989). This shows the importance of taking ionization

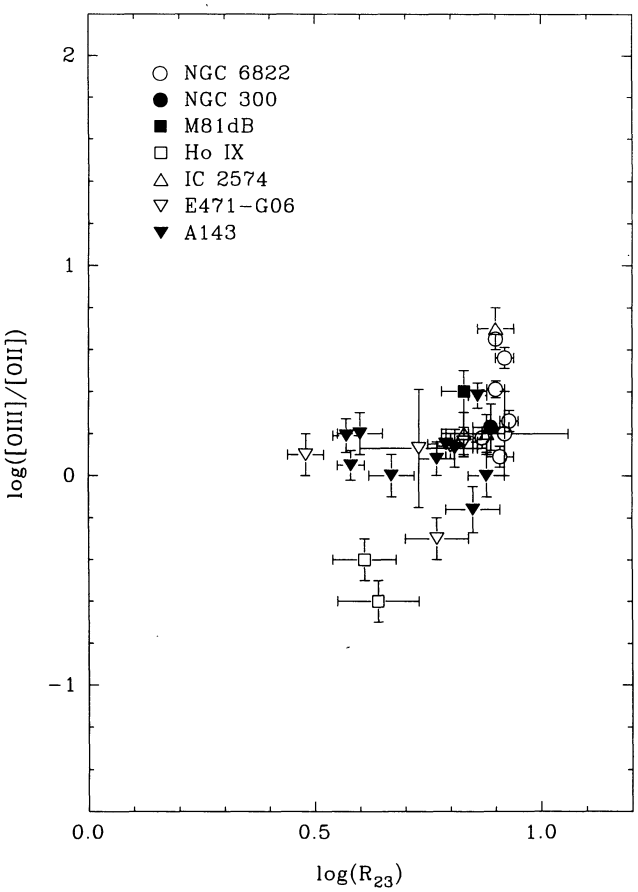

FIG. 5.—Log ([O III]/[O II]) vs. log (R_{23}) for the H II regions in the Sculptor and M81 Group dwarf galaxies. In conjunction with Fig. 2 of McGaugh (1994), this plot can be used to determine log (U) and log (O/H). Data points for NGC 6822, NGC 300 and the Sculptor dwarfs E471-G06 and A143 are from Miller (1996). Points for Ho IX are from Miller (1995).

into account. Low-abundance H II regions do not necessarily have high ionizations, as one would expect from the model that stars with low abundances are hotter than stars with high abundances and that low-abundance nebulae cool less efficiently.

3.4. *Nitrogen Abundances*

One can infer the nitrogen abundance directly from the [N II] λ6584/[O II] λ3727 ratio. While the ionization correction factor (ICF) between N^+/O^+ and N/O can be quite large at solar metallicity, it is reasonable to assume that $N/O = N^+/O^+$ for low-metallicity H II regions (Garnett 1990). Table 2 shows that $\log (N/O) = -1.26 \pm 0.25$ for M81dB and -1.53 ± 0.02 for IC 2574. These numbers agree with the range of nitrogen abundances in other nearby irregular galaxies (Garnett 1990).

3.5. *Reddening*

The logarithmic extinction at Hβ, $c(H\beta)$, is related to the reddening, $E(B-V)$, according to

$$E(B-V) = \frac{c(H\beta)}{0.4(R+0.53)} \quad (3)$$

for the parameterization of the extinction law that we are using (Howarth 1983). A value of $R = 3.1$ is being assumed. Reddenings calculated using equation (3) are shown in the last row of Table 2. For Ho I and M81dB the reddening is consistent with zero, but in IC 2574 the reddening is larger than the total reddening (Galactic plus correction to face-on) given in the RC3. This extra absorption may be due to additional dust in the H II regions.

4. DISCUSSION

SKH have shown that there is a convincing correlation between the logarithm of the oxygen abundance and the absolute blue magnitude of the galaxy (see Fig. 6). Using the absolute magnitudes from MH94, the range of abundances using both the upper and lower branches for the current sample of galaxies are also plotted in Figure 6. In all cases, the lower branch abundances match the overall trend better than the upper branch abundances. This supports the conclusion reached using the [N II]/[O II] ratio that all these galaxies are typical, low-abundance dwarfs. Despite a spread in absolute magnitude of about 4.5 mag, the lower branch abundances of the three galaxies are essentially identical at $12 + \log O/H) \sim 8.0$, or 12% of solar.

Some comments on the individual galaxies follow.

Ho I.—The one spectrum of the brightest H II region in this galaxy was taken through significant cloud cover so that the [O II] λ3727 line was not even detected (see Fig. 1). In Table 1 we report an upper limit [O II] λ3727 flux and use that to determine the oxygen abundance. The lower branch abundance relation gives an upper limit to the oxygen abundance of $5^{+5}_{-2.5} \times 10^{-5}$ [$12 + \log (O/H) = 7.7 \pm 0.3$]. Using EP's lower branch calibration of [O III](4959 + 5007) with $12 + \log (O/H)$ also gives $12 + \log (O/H) \approx 7.7 \pm 0.2$ or $O/H = 5 \pm 3 \times 10^{-5}$. While this agreement is encouraging, better observations are needed to detect [O II] λ3727 and reduce the uncertainties.

M81dB.—M81dB (or UGC 5423) is the lowest luminosity galaxy in the current sample for which a spectrum has been obtained, and it does seem to fall convincingly on the lower branch of the R_{23} relation. There is a weak [O III] λ4363 detection, which gives $O/H = 9.5 \pm 4.5 \times 10^{-5}$, in good agreement with $O/H = 7.9 \pm 1.8 \times 10^{-5}$ from the lower branch calibration. These results are also in reasonable agreement (within 2 σ) with the value of $O/H = 5.5 \times 10^{-5}$ from Skillman et al. (1993). Our abundance puts M81dB on the upper envelope of the log (O/H)–M_B relation. M81dB is currently undergoing a starburst and we may be seeing oxygen enriched gas from recent supernovae or stellar winds (Lequeux et al. 1981; Kunth & Sargent 1986; Garnett 1990). The slightly enhanced N/O ratio compared to IC 2574 may give some support to this hypothesis. Another problem may be that the absolute blue magnitude that we adopted is too large, either because the distance is substantially different from that of M81 or because of a systematic error in the photometry. An independent distance estimate and new CCD photometry of this galaxy are needed to resolve this.

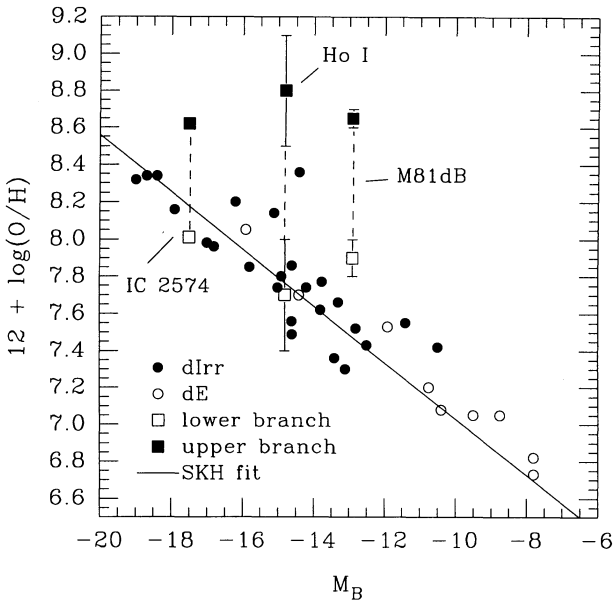

FIG. 6.—Trend of log (O/H) with the absolute blue magnitude for nearby dwarf irregular galaxies. The filled circles are from Skillman et al. (1993), open circles are from SKH. The solid line is the least-squares fit from SKH. Open and filled squares are for the galaxies in this study and indicated lower and upper branch abundances, respectively. Error bars represent either the range of metallicities for galaxies with abundance measurements from several H II regions or the error in individual measurements.

IC 2574.—This galaxy has the highest luminosity in the sample and, like the LMC, it is probably more correct to consider it an Irr galaxy than a dIrr galaxy. The spectrograph slit was placed on the peak of the bright H II region complex at the north end of the bar (Fig. 3 of MH94) and fell across three bright H II regions. The [O III] λ4363 line was detected in region 167 and it gives temperatures of 14,400 K and oxygen abundances of 1.4×10^{-4}, in good agreement with the abundances from the lower branch calibration. As can be seen in Figure 6, IC 2574 is consistent with the log (O/H)–M_B relation of SKH.

4.1. *Summary*

Long-slit spectroscopy of the brightest H II regions in Ho I, M81dB, and IC 2574 has been presented and oxygen abun-

dances calculated using a combination of direct and empirical methods. All of these galaxies fall on the lower branch of the log (O/H), R_{23} empirical abundance relation and have oxygen abundances $\leq 12\%$ of solar. The H II regions also have relatively low excitation. The N/O ratios are typical for dwarf galaxies and the slightly larger N/O ratio in M81dB, compared with IC 2574, may indicate an enhancement from stellar winds or supernovae. These abundances are important pieces of information for unraveling the star formation histories of these galaxies. Higher resolution spectra of any of these galaxies could be useful for addressing the question of the primordial helium abundance.

We would like to thank the KPNO TAC for allocation of telescope time and the KPNO staff for their assistance. We are also grateful to Evan Skillman for useful discussions. This work was partially supported by National Science Foundation grant 92-15821 to Paul Hodge.

REFERENCES

Brocklehurst, M. 1971, MNRAS, 153, 471
De Robertis, M. M., Dufour, R. J., & Hunt, R. W. 1987, JRASC, 81, 195
Drissen, L., Roy, J. R., & Moffat, A. F. J. 1993, AJ, 106, 1460
Edmunds, M. G., & Pagel, B. E. J. 1984, MNRAS, 211, 507 (EP)
Gallagher, J. S., & Hunter, D. A. 1984, ARA&A, 22, 37
Garnett, D. R. 1990, ApJ, 363, 142
Garnett, D. R., Skillman, E. D., Dufour, R. J., Peimbert, M., Torres-Peimbert, S., Terlevich, R., Terlevich, E., & Shields, G. A. 1995, ApJ, 443, 64
Gilmore, G., & Wyse, R. F. G. 1991, ApJ, 367, L55
Hodge, P., & Miller, B. W. 1995, ApJ, 451, 176
Howarth, I. D. 1983, MNRAS, 203, 301
Hunter, D. A., & Gallagher, J. S. 1985, ApJS, 58, 533
Kunth, D., & Sargent, W. L. W. 1986, ApJ, 300, 496
Lequeux, J., Maucherat-Joubert, M., Deharveng, J. M., & Kunth, D. 1981, A&A, 103, 305
McGaugh, S. S. 1991, ApJ, 380, 140
———. 1994, ApJ, 426, 135
Miller, B. W. 1995, ApJ, 446, L75
———. 1996, AJ, submitted
Miller, B. W., & Hodge, P. 1994, ApJ, 427, 656 (MH94)
Pagel, B. E. J., Edmunds, M. G., Blackwell, D. E., Chun, M. S., & Smith, G. 1979, MNRAS, 189, 95
Pagel, B. E. J., Simonson, E. A., Terlevich, R. J., & Edmunds, M. G. 1992, MNRAS, 255, 325
Seaton, M. J. 1979, MNRAS, 187, 73P
Shields, G. A. 1990, ARA&A, 28, 525
Skillman, E. D. 1989, ApJ, 347, 883
Skillman, E. D., & Kennicutt, R. C. 1993, ApJ, 411, 655
Skillman, E. D., Kennicutt, R. C., & Hodge, P. W. 1989, ApJ, 347, 875 (SKH)
Skillman, E. D., Melnick, J., Terlevich, R., & Moles, M. 1988, A&A, 196, 31
Skillman, E. D., Terlevich, R. J., Kennicutt, R. C., Garnett, D. R., & Terlevich, E. 1994, ApJ, 431, 172
Skillman, E. D., Terlevich, R. J., Terlevich, E., Kennicutt, R. C., & Garnett, D. R. 1993, in Texas/PASCOS 92 Relativistic Astrophysics and Particle Cosmology, ed. C. Akerlof & M. Srednicki (New York: New York Acad. Sci.), 739
Stasińska, G. 1982, A&AS, 48, 299
———. 1990, A&AS, 83, 501